

# Kinetic Comparison of the Specificity of the Vancomycin Resistance Kinase VanS for Two Response Regulators, VanR and PhoB<sup>†</sup>

Stewart L. Fisher,<sup>‡</sup> Soo-Ki Kim,<sup>§</sup> Barry L. Wanner,<sup>§</sup> and Christopher T. Walsh<sup>\*‡</sup>

Department of Biological Chemistry and Molecular Pharmacology, Harvard Medical School, Boston, Massachusetts 02115, and Department of Biological Sciences, Purdue University, West Lafayette, Indiana 47907

Received October 25, 1995; Revised Manuscript Received January 24, 1996<sup>®</sup>

**ABSTRACT:** Induction of vancomycin resistance in the Gram-positive *Enterococci* requires a two-component regulatory system, VanS and VanR, for transcriptional activation of three genes (*vanH*, *A*, *X*) that encode enzymes for a cell wall biosynthetic pathway that produces an altered peptidoglycan intermediate with lower affinity for the antibiotic. The catalytic efficiency ( $k_{\text{cat}}/K_M$ ) has been determined for phosphotransfer from the phosphohistidyl form of VanS to both its homologous partner VanR and the heterologous (*Escherichia coli*) response regulator PhoB. The rate of formation of the phosphoaspartyl forms of VanR and PhoB were determined as well as the rate of appearance of inorganic phosphate. Using PhoB in excess of P-VanS, a pseudo-first-order rate constant ( $k_{\text{xfer}}$ ) of  $0.2 \text{ min}^{-1}$  for phosphotransfer and a  $K_M$  for PhoB of  $100 \mu\text{M}$  were readily determined. The corresponding  $k_{\text{xfer}}$  of  $96 \text{ min}^{-1}$  for phosphotransfer from P-VanS to VanR required rapid quench kinetics. A  $K_M$  of  $3 \mu\text{M}$  was estimated for VanR, leading to a  $10^4$ -fold preference in  $k_{\text{xfer}}/K_M$  for phosphotransfer to VanR compared to PhoB. No phosphotransfer was detectable to three other *E. coli* response regulators, OmpR, ArcB, or CreB, providing some sense of the selectivity against two-component regulatory system cross-talk. In the phosphotransfer from P-VanS to PhoB and VanR, there was evidence of competition between water, to give  $\text{P}_i$ , and the specific aspartyl  $\beta\text{-COO}^-$  moiety of either PhoB or VanR, with about 25% of the initial flux generating inorganic phosphate. The kinetics of phosphotransfer from P-VanS to VanR were complicated by inhibition by free VanS, but the inhibition pattern could be modeled to yield a  $K_D$  of  $30 \text{ nM}$  for VanR binding to free VanS, an affinity similar to that of the CheA-CheY pair in *E. coli* chemotaxis.

Vancomycin is a glycopeptide antibiotic that has been in clinical use for over 30 years for the treatment of Gram-positive bacterial infections (Wilhelm, 1991). Vancomycin induces cell death by osmotic shock since it binds to the terminal D-Ala-D-Ala moieties of the bacterial cell wall and effectively inhibits the transpeptidation and transglycosylation steps of the cell wall assembly process (Nagarajan, 1991). Although vancomycin has remained relatively free from widespread resistance problems, a number of *Enterococci* strains with high level resistance to vancomycin have been identified recently (Hakenbeck, 1994). High-level resistance to the drug has been found to require five plasmid-borne genes: *vanH*, *vanA*, *vanX*, *vanR*, and *vanS*.

VanS and VanR comprise a two-component regulatory system (Arthur et al., 1992; Wright et al., 1993) that regulates the transcriptional activation of the genes responsible for conferring resistance: *vanH*, *vanA*, and *vanX* (Wright & Walsh, 1992). Two-component regulatory systems are signal transduction pathways commonly used by prokaryotes to sense and adapt to stimuli in the environment; as many as 50 different ones may exist in a bacterium such as *Escherichia coli* (Parkinson & Kofoed, 1992; Parkinson, 1993). In

addition, analogous signal transduction pathways have recently been identified in both eukaryotes (Swanson et al., 1994) and archaea (Rudolph et al., 1995). These systems are characterized by a sensor kinase (often a transmembrane signaling kinase such as VanS) that undergoes autophosphorylation on a histidine residue. This phosphoryl group is then transferred to an aspartate residue on a response regulator protein (in this case, VanR) that usually acts as a transcriptional activator. Like many signaling kinases, VanS has an N-terminal domain with two membrane-spanning segments believed to act as a signal sensing domain and a C-terminal cytoplasmic "transmitter" domain with autophosphorylation and phosphotransfer activities. Biochemical studies on the cytoplasmic domain of VanS (M95-S384) have shown that it is readily autophosphorylated at a histidine residue (H164) in the presence of ATP and that P-VanS<sup>1</sup> is capable of efficient phosphotransfer to an aspartate residue on VanR (D53) (Wright et al., 1993). Genetic studies have implicated VanR as a transcriptional activator of the vancomycin resistance genes (Arthur et al., 1992). These predictions have been borne out by *in vitro* studies with the purified protein. Gel-mobility shift and DNase footprinting analyses have shown that P-VanR has an enhanced binding affinity for the  $P_{\text{vanH}}$  and  $P_{\text{vanR}}$  promoter regions of the vancomycin resistance operon (Holman et al., 1994).

<sup>†</sup> This research was supported by NIH Grant GM35392 to B.L.W. and by NIH Grant GM49338 to C.T.W. S.L.F. was supported by a National Institutes of Health Post-Doctoral Fellowship (NIH GM16259).

\* To whom correspondence should be addressed.

<sup>‡</sup> Harvard Medical School.

<sup>§</sup> Purdue University.

<sup>®</sup> Abstract published in *Advance ACS Abstracts*, April 1, 1996.

<sup>1</sup> Abbreviations: BSA, bovine serum albumin; IPTG, isopropyl  $\beta$ -D-thiogalactopyranoside; MBP, maltose binding protein; PAGE, polyacrylamide gel electrophoresis; PMSF, phenylmethanesulfonyl fluoride; P-PhoB, phospho-PhoB; SDS, sodium dodecyl sulfate; P-VanR, phospho-VanR; P-VanS, phospho-VanS.

In addition to activation of VanR, the cytoplasmic domain of VanS was recently found to be capable of *in vivo* activation and *in vitro* phosphorylation of the *E. coli* response regulator PhoB (Fisher et al., 1995). In wild-type cells, PhoB, together with its cognate sensor kinase PhoR, control the expression of the Pho regulon in response to phosphate limitation (Wanner, 1993). This cross-reactivity between VanS and PhoB provides a sensitive *in vivo* assay for VanS activation and allows for genetic analyses of the factors that regulate two-component system signal transduction. In addition, the ability to compare the relative reactivities of the two response regulator proteins *in vitro* provides an opportunity to begin to define and quantify the elements that govern specificity between the multitude of signal transduction systems present in a single cell. In this regard, preliminary *in vitro* investigations indicated that VanR and PhoB exhibited at least a >100-fold difference in reactivities toward P-VanS (Fisher et al., 1995). In this work, we undertook a comprehensive kinetic investigation of the phosphotransfer reactivities of the two response regulators. We found that both PhoB and VanR are well-behaved, saturable substrates for P-VanS; however, the two response regulators differ by >10<sup>4</sup>-fold in their relative catalytic efficiency for phosphotransfer. In addition, the phosphotransfer reactions for the two proteins exhibit a phosphate hydrolysis pathway which suggests that the chemical transfer step between the two proteins can be intercepted by water.

## MATERIALS AND METHODS

**General Methods.** ATP was purchased from Boehringer Mannheim, and [ $\gamma$ -<sup>32</sup>P]ATP was purchased from Dupont NEN. Protein concentrations were measured using either the Bio-Rad Protein Assay (Hercules, CA) using bovine serum albumin as a standard or spectrophotometrically using the method of von Hippel (Gill & von Hippel, 1989). Measurements made using the Bio-Rad Protein Assay were found to be 1.8–2.0-fold lower than those obtained spectrophotometrically and were corrected accordingly. All experiments were carried out at 25 °C unless otherwise noted. All experiments were performed at least twice. The reported data represents the average of the multiple runs; for those reactions run three or more times, the error bars represent the standard error of the mean. Kinetic constants were calculated using the general curve fitting options in Kaleidagraph v. 3.0.1 (Synergy Software, Reading, PA) on a MacIntosh Quadra computer (Apple Computer, Inc., Cupertino, CA).

**Preparation of Overproducing Constructs.** The plasmid pSK5 carries the *E. coli* *phoB* gene as an *Nde*I to *Bam*HI fragment in pET22b(+) (Novagen, Madison, WI). It was made in three steps. First, a 4.8 Kb *Eco*RI to *Hin*DIII fragment carrying the *phoBR* operon was cloned from pBC6DPsI [a derivative of pBC6 deleted of an upstream *Pst*I fragment (Wanner & Chang, 1987)] into the polylinker of pBGS131(+) (Spratt et al., 1986). The new plasmid was named pSK1. The translational start codon was then changed to an *Nde*I site, and a *Bam*HI site was introduced within the *phoB*-to-*phoR* intergenic regions by site-directed mutagenesis (Kunkel, 1985) using the oligonucleotides 5'-TACGTCTCGC-CATATGTTGCCCTGTTGTAA-3' and 5'-TAAGCCCTGCTCTGGATCCGATGAGCAAGG-3', respectively. A plasmid carrying both new restriction sites was named pSK2,

and these regions were verified by DNA sequencing with primers complementary to *phoB* and *phoR* sequences. Subsequently, the 0.7 kb *Nde*I to *Bam*HI fragment carrying the *phoB* region of pSK2 was subcloned into pET-22b(+). pSK5 was transformed into *E. coli* BL21(DE3) (Studier, 1991) for protein production.

**Purification of Proteins.** VanR and MBP-VanS were purified as described previously to >95% purity as assessed by Coomassie Brilliant Blue-stained SDS-PAGE gels (Wright et al., 1993). Purification of PhoB protein was accomplished by subculturing (1:100) a saturated culture of *E. coli* BL21(DE3)/pSK5 into 1 L of Luria-Bertini broth (1% tryptone, 1% NaCl, and 0.5% yeast extract) containing ampicillin (100  $\mu$ g/mL) followed by incubation at 37 °C with agitation. When the culture reached an OD<sub>595nm</sub>  $\approx$  0.4–0.6, IPTG was added to a final concentration of 1 mM, and the cells were grown for an additional 2 h. Cells were harvested by low-speed centrifugation (2500g, for 10 min) and resuspended in 20 mL of lysis buffer [50 mM Tris, pH 7.4, 300 mM NaCl, 5 mM MgCl<sub>2</sub>, PMSF (0.0001%), leupeptin (1  $\mu$ g/mL), and chymostatin (1  $\mu$ g/mL)]. The cells were disrupted by two passages through a French pressure cell (15 000 psi), and cell debris was removed by centrifugation (25000g, for 30 min). The supernatant was brought to 50% saturation in ammonium sulfate, nutated for 1 h at 4 °C, and then centrifuged (25000g, for 30 min). The resulting pellet was resuspended in 3 mL of buffer A (50 mM Bis-Tris, pH 7.4, 50 mM NaCl, 5 mM MgCl<sub>2</sub>) and loaded onto an Ultragel Aca54 (LKB) gel filtration column (100  $\times$  2.5 cm) at 4 °C. Proteins were eluted with buffer A (1 mL/min), and fractions containing PhoB (analyzed using SDS-PAGE) were combined and loaded onto a Resource-Q column (1  $\times$  10 cm, Pharmacia Biotech, Piscataway, NJ) using buffer A and eluted with a linear gradient of NaCl (50–750 mM). Only a small fraction of the PhoB protein was bound on the first passage through the column; however, most of the protein bound and subsequently eluted at  $\approx$ 230 mM NaCl after reloading the PhoB-containing fractions from the first passage. Fractions containing pure PhoB (>95%, as determined by SDS-PAGE with Coomassie Brilliant Blue staining) were combined and concentrated to  $\approx$ 3 mg/mL protein using Centriprep-10 concentrators (Amicon, Inc., Beverly, MA). Protein stocks were brought to 20% glycerol and stored at –80 °C. Gel filtration analysis of the purified protein, using a Sephadex-75 column (Pharmacia) and buffer B (50 mM Tris, pH 8.0, 1 mM MgCl<sub>2</sub>, 200 mM NaCl; 0.5 mL/min), was consistent with a monomeric protein of correct molecular weight (estimated molecular mass  $\approx$ 31 kDa; predicted molecular mass = 26.4 kDa, data not shown).

**Purification of Phosphorylated Proteins.** Purified P-MBP-VanS was prepared as described previously by multiple washes using a Microcon-30 concentrator (Amicon Inc., Beverly, MA) (Fisher et al., 1995). In all cases, P-MBP-VanS was found to comprise  $\approx$ 10% of the total MBP-VanS present, consistent with the previous report (Wright et al., 1993). P-PhoB was prepared by incubating purified P-MBP-VanS (100 pmol) and PhoB (4 nmol) in 100  $\mu$ L of buffer C (50 mM Tris, pH 7.4, 50 mM KCl, 1 mM MgCl<sub>2</sub>) at 30 °C for 20 min. The solution was then loaded on an amylose column (0.25  $\times$  1 cm) pre-equilibrated with buffer D (50 mM Tris, pH 8.0, 50 mM NaCl, 5 mM EDTA). Fractions containing PhoB were identified by Bio-Rad Protein Assay,

pooled, and then concentrated to  $\approx 50 \mu\text{L}$  in a Microcon-10 concentrator. The protein solution was then diluted to 0.5 mL with buffer D and subsequently concentrated again in a Microcon-10 concentrator. This process was repeated an additional four times to remove the residual radioactive inorganic phosphate ( $\text{P}_i$ ); however, the final wash was performed with buffer C. As expected, the recovered P-PhoB protein was found to comprise  $\approx 15\%$  of the total PhoB present.

**Phosphotransfer Time Course Experiments:** (a) *PhoB*. Phosphotransfer from [ $^{32}\text{P}$ ]MBP-VanS to PhoB was initiated by the addition of [ $^{32}\text{P}$ ]MBP-VanS (2 nmol) to a solution of PhoB (8 nmol) in 100  $\mu\text{L}$  of buffer C. At designated time points, aliquots (6  $\mu\text{L}$ ) of the reaction mixture were removed and quenched with SDS stop buffer (4  $\mu\text{L}$  of 125 mM Tris, pH 6.8, 2.5% SDS, 2 mM EDTA, 0.0025% bromophenol blue, and 25% glycerol). The quenched solutions were run on 12% SDS-PAGE, and the  $^{32}\text{P}$ -labeled gels were frozen at  $-80^\circ\text{C}$  to prevent diffusion of radioactive  $\text{P}_i$ . Radioactive species were analyzed using phosphorimager (Molecular Dynamics Inc., Sunnyvale, CA or Fuji Medical Systems, USA, Stamford, CT). Quantification of the labeled species was calculated as relative proportions of the total counts in a given gel lane. The total counts in each lane were normalized to an arbitrary value for each gel to correct for variations in sample loading. Actual concentrations of the radioactive species were calculated from the initial concentration of [ $^{32}\text{P}$ ]MBP-VanS.

(b) *VanR*. Phosphotransfer to VanR on long time scales (15 s to 4 h) was carried out as described above for PhoB; in these experiments VanR and [ $^{32}\text{P}$ ]MBP-VanS were at 15 and 0.5  $\mu\text{M}$ , respectively. For those reactions run on short time scales ( $< 15$  s), rapid chemical quench techniques were employed. For these experiments, 20  $\mu\text{L}$  of a VanR stock (30  $\mu\text{M}$  in buffer C) and 20  $\mu\text{L}$  of a [ $^{32}\text{P}$ ]MBP-VanS stock (10  $\mu\text{M}$  in buffer C) were mixed in a Quench-Flow apparatus (Kintech Co., State College, PA) for a specified length of time and then quenched with 60  $\mu\text{L}$  of quench buffer (75 mM Tris, pH 8.0, 0.6% SDS, 1.2 mM EDTA, 0.0025% bromophenol blue, and 15% glycerol). The resulting quenched solutions were loaded on a 12% SDS-PAGE gel (five-well) and quantified using phosphorimage analysis as described above. It was observed that EDTA alone was not sufficient to stop the reaction progress; it was necessary to add SDS in the quench solution to obtain reproducible results on this time scale.

(c) *Dephosphorylation of PhoB*. P-PhoB dephosphorylation in the absence of VanS was monitored by quenching aliquots (6  $\mu\text{L}$ ) of a P-PhoB solution (0.15  $\mu\text{M}$ ) in buffer C at designated intervals in SDS stop buffer (4  $\mu\text{L}$ ). To study the effect of VanS on dephosphorylation rate, P-PhoB solutions (0.6  $\mu\text{M}$ ) containing MBP-VanS (45  $\mu\text{M}$ ) were prepared under identical conditions. In both cases, the radioactive species were quantified using SDS-PAGE and phosphorimage analysis as described above.

**Measurement of Kinetic Constants:** (a) *PhoB*. Aliquots (1.5  $\mu\text{L}$ , 1  $\mu\text{M}$ ) of [ $^{32}\text{P}$ ]MBP-VanS were added to stock solutions of PhoB (13.5  $\mu\text{L}$ , 11–111  $\mu\text{M}$ ) in buffer C and incubated at  $25^\circ\text{C}$ . These reactions were quenched with 5  $\mu\text{L}$  of SDS stop buffer when 10–15% of the initial [ $^{32}\text{P}$ ]MBP-VanS had transferred phosphate to PhoB (30 s to 3 min; accumulation of P-PhoB was found to be essentially linear up to 15% accumulation for this range of concentra-

tions). After quantification of the radioactive species using SDS-PAGE and phosphorimage analysis, the kinetic constants were calculated using nonlinear least-squares regression curve fitting to a rectangular hyperbola.

(b) *VanR*. Reactions were carried out using rapid chemical quench techniques as described above for the phosphotransfer time course; however, stock solutions of [ $^{32}\text{P}$ ]MBP-VanS (0.25  $\mu\text{M}$ , 2.25  $\mu\text{M}$  MBP-VanS) and VanR stock solutions ranging from 0.5 to 30  $\mu\text{M}$  were employed. Reaction times were chosen such that 10–15% of the initial [ $^{32}\text{P}$ ]MBP-VanS had transferred phosphate to VanR for all concentrations of VanR (75 ms to 5 s). The data were fitted using nonlinear regressions to a model which included inhibition by VanR depletion through nonproductive binding to the free VanS present in the  $^{32}\text{P}$ -MBP-VanS preparation (Segel, 1993). In this case the reaction velocity is expressed as

$$v = \frac{V_{\max}[\text{VanR}_{\text{free}}]}{K_{\text{VanR}} + [\text{VanR}_{\text{free}}]}$$

where

$$[\text{VanR}_{\text{free}}] = \{([\text{VanS}] - [\text{VanR}] + K_{\text{VanS/R}})^2 - 4K_{\text{VanS/R}}[\text{VanS}] - ([\text{VanS}] - [\text{VanR}] + K_{\text{VanS/R}})\}^{1/2}/2$$

**PhoB Inhibition.** To study the PhoB inhibition of the P-VanS to VanR phosphotransfer, reactions were run as described above with the addition of PhoB (10–80  $\mu\text{M}$ ) to the VanR stocks (1–2.5  $\mu\text{M}$ ). Reaction times for these experiments were 75 ms. Control experiments verified that [ $^{32}\text{P}$ ]PhoB was not formed under these conditions.

**Kinetic Simulations.** Kinetic simulations were performed using numerical integration with the program Kinsim v3.3 (Barshop et al., 1983) on a Silicon Graphics Iris 4D/20 workstation (Mountain View, CA).

## RESULTS

**Preparation of Protein Substrates.** The kinetic studies presented in this work required high-yielding overproduction systems and efficient purification strategies to prepare sufficient quantities of both the sensor kinase VanS and the response regulator proteins VanR and PhoB. To this end, the sensor kinase VanS was prepared as a maltose binding protein fusion to the C-terminal cytoplasmic domain (residues M95-S384), since this approach afforded large quantities ( $> 100$  mg of protein/L) of soluble, purified protein. In addition, previous work on MBP-VanS has shown that it readily undergoes autophosphorylation with ATP and the subsequent phosphorylated form is stable to purification (Wright et al., 1993). Further, the phosphorylated form can transfer the phosphate group to both VanR and PhoB (Wright et al., 1993; Fisher et al., 1995). However, for reasons that are still unclear, autophosphorylation of the MBP-VanS protein proceeds to load only  $\approx 10\%$  of the total protein with phosphate, even under conditions of saturating ATP and extended reaction times. Attempts to purify the phosphorylated protein from the free MBP-VanS have proven unsuccessful, and, as a result, the P-MBP-VanS used in these studies contained contaminating levels of the free protein in a 1:9 mixture. Both PhoB and VanR were prepared as the full-length proteins. Large quantities of these proteins were necessary, since both VanR and PhoB were always main-

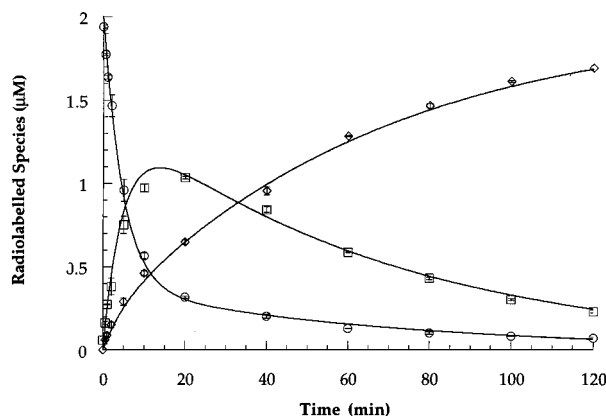


FIGURE 1: Time course of phosphotransfer from  $^{32}\text{P}$ -VanS to PhoB. Reactions were run and analyzed using SDS-PAGE and phosphorimage analysis as described in Materials and Methods; data at designated time points represent  $^{32}\text{P}$ -labeled species: (○) P-MBP-VanS; (□) P-PhoB, and (◇)  $\text{P}_i$ . Initial concentrations of the reactants were as follows: MBP-VanS,  $18\ \mu\text{M}$ ; P-MBP-VanS,  $2\ \mu\text{M}$ ; PhoB,  $40\ \mu\text{M}$ . Solid lines represent computer simulations according to the phosphotransfer model (see eq 3). Simulations were run with the following kinetic constant values:  $K_{\text{M,PhoB}} = 100\ \mu\text{M}$ ;  $k_2 = 0.20\ \text{min}^{-1}$ ;  $k_{-2} = 0.05\ \text{min}^{-1}$ ;  $k_3 = 1.25\ \text{min}^{-1}$ ;  $k_{-3} = 0.05\ \mu\text{M}^{-1}\ \text{min}^{-1}$ ;  $k_4 = 0.06\ \text{min}^{-1}$ ;  $k_5 = 0.015\ \text{min}^{-1}$ ;  $k_6 = 0.011\ \text{min}^{-1}$ . Rate constants  $k_{-2}$ ,  $k_3$ , and  $k_{-3}$  were derived empirically and found to be relatively insensitive to the overall fit; all other constants were measured as described in Materials and Methods.

tained in stoichiometric excess of the P-VanS to allow quantitative transfer of the phosphate group to the response regulator. The VanR overproduction and purification strategies employed for previous studies (Wright et al., 1993) provided sufficient material for this work. Overproduction of full-length PhoB was achieved using a T7-based expression system which provided ample soluble protein ( $>50\ \text{mg/L}$ ). Purification of PhoB to homogeneity followed a strategy similar to that used for VanR.

We used a modified version of the radioactive SDS-PAGE and phosphorimage analysis assay reported by Morrison and Parkinson (1994) developed for the CheA-CheY two-component regulatory system. In our studies, we found that exposing the radioactively labeled, wet polyacrylamide gels on phosphorimager plates at  $-80\ ^\circ\text{C}$  prevented diffusion of the inorganic phosphate and allowed extended exposure times ( $>24\ \text{h}$ ) for signal enhancement. Using this assay, we typically found backgrounds that were 0.5% of the total quantified labeled species, and duplicate samples were generally within 15%.

**Phosphotransfer Kinetics from  $^{32}\text{P}$ -VanS to PhoB.** We initiated our studies with PhoB, since preliminary investigations on the phosphotransfer between VanS and PhoB demonstrated that the transfer reaction occurred on a time regime slow enough for conventional analysis. The time course for phosphotransfer from  $^{32}\text{P}$ -VanS to PhoB is shown in Figure 1. By inspection of the time course, it is clear that the overall transfer follows a biphasic process. In the early stage of the phosphotransfer (0–20 min),  $^{32}\text{P}$ -VanS rapidly decays with a concomitant increase in both  $^{32}\text{P}$ -PhoB and inorganic phosphate ( $^{32}\text{P}_i$ ), to give a maximal loading of PhoB to approximately 55% of the initial  $^{32}\text{P}$ -VanS concentration. The second phase of the phosphotransfer is characterized by a slow decay of both labeled proteins with a corresponding accumulation of  $\text{P}_i$ . Studies on the related chemotaxis two-component system have invoked a simple model (eq 1) for describing the phosphotransfer processes

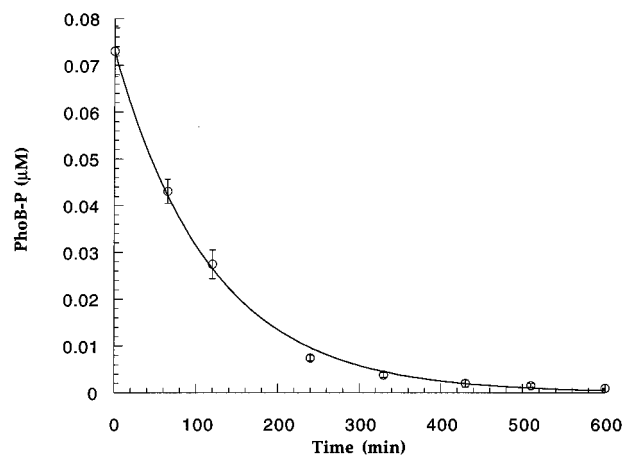
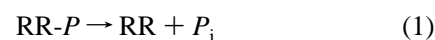
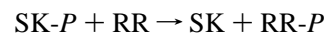


FIGURE 2: Autodephosphorylation of P-PhoB. Reactions were run as described in Materials and Methods; The data were fit to a single-exponential decay (solid line).



between the kinase CheA and the response regulator CheY (Lukat et al., 1991; Bray et al., 1993; Morrison & Parkinson, 1994; Hauri & Ross, 1995). The model predicts a simple bimolecular reaction between the two proteins with phosphate release arising from the autodephosphorylation of the phosphorylated response regulator. There are several aspects of the P-VanS to PhoB phosphotransfer time course that are inconsistent with this model, the first of which involves the accumulation of  $\text{P}_i$  in the early stages of the reaction. A comparison of the inorganic phosphate accumulation with the P-PhoB formation curve suggests that the rate of phosphate generation is  $\approx 25\%$  that of the corresponding P-PhoB formation. This initial burst of phosphate is unlikely to be derived primarily from dephosphorylation of P-PhoB, as autodephosphorylation from this species alone would require a lag phase in phosphate production while the P-PhoB was accumulating. Thus, a sigmoidal phosphate production curve would be expected.

In order to further investigate the rates of phosphate hydrolysis in these studies, we prepared  $^{32}\text{P}$ -labeled P-PhoB. This product was prepared from reactions with purified [ $^{32}\text{P}$ ]-MBP-VanS followed by purification of the product through affinity chromatography (to remove MBP-VanS) and extensive washing (to remove low molecular weight radioactive species). As expected, P-PhoB dephosphorylated exponentially with time in the presence of  $\text{Mg}^{2+}$  (see Figure 2;  $k_{\text{dephos}} = 8.5 \times 10^{-3} \pm 0.2 \times 10^{-3}\ \text{min}^{-1}$ ). This dephosphorylation was dependent on  $\text{Mg}^{2+}$ ; in the absence of this cation there was no detectable dephosphorylation over a similar time frame (10 h). The autodephosphorylation of some response regulators has also been found to be enhanced in the presence of the sensor kinase (Tokishita et al., 1992; Kamberov et al., 1994). On the basis of this precedent, we tested whether VanS had such an effect on P-PhoB. The addition of VanS ( $40\ \mu\text{M}$ ) to P-PhoB ( $1\ \mu\text{M}$ ) had a minimal effect on the overall dephosphorylation (Figure 3), only increasing the rate 1.5-fold ( $k_{\text{dephos}} = 1.2 \times 10^{-2} \pm 0.1 \times 10^{-2}\ \text{min}^{-1}$ ). The fact that VanS has such a small effect on the P-PhoB stability suggests that an alternative pathway exists for dephosphorylation in the phosphotransfer reaction starting from P-VanS.

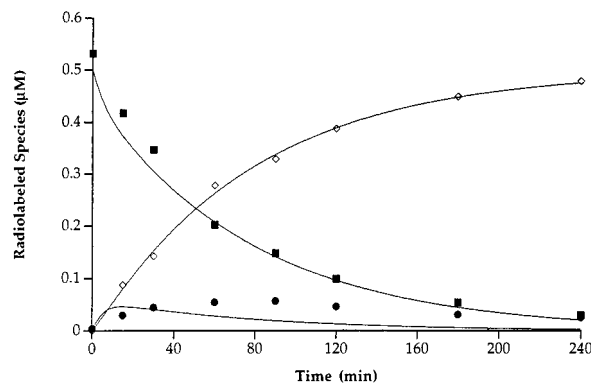
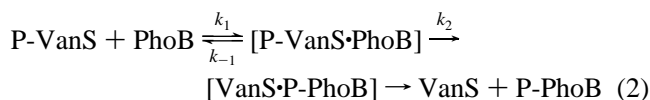


FIGURE 3: Time course of phosphotransfer from  $^{32}\text{P}$ -PhoB to VanS. Reactions were run and analyzed using SDS-PAGE and phosphorimage analysis as described in Materials and Methods; data at designated time points represent  $^{32}\text{P}$ -labeled species: (●) P-MBP-VanS; (■) P-PhoB, and (◇)  $\text{P}_i$ . Initial concentrations of the reactants were as follows: MBP-VanS, 40  $\mu\text{M}$ ; PhoB, 0.9  $\mu\text{M}$ ; P-PhoB, 0.1  $\mu\text{M}$ ; active MBP-VanS was assumed to be  $\approx 10\%$  of the total concentration based on the autophosphorylation activity. Solid lines represent computer simulations according to the phosphotransfer model (see eq 3) with the identical kinetic constant values to those used in Figure 1.

The simple model proposed for phosphotransfer between the kinase and response regulator proteins (eq 1) also predicts that the reaction follows a bimolecular process. We tested this hypothesis on the P-VanS to PhoB phosphotransfer reaction by investigating the rate dependence of the phosphotransfer reaction on the PhoB concentration under initial conditions. In these experiments, the rate of formation of P-PhoB was measured in conditions where PhoB was in large excess to the  $^{32}\text{P}$ -VanS ( $\geq 10$ -fold), and the reaction was only allowed to proceed to achieve  $\approx 10\%$  accumulation of the P-PhoB product ( $\leq 20\%$  P-VanS consumed). The system was well behaved kinetically; accumulation of P-PhoB was found to be essentially linear to  $\approx 20\%$  total P-PhoB for all of the concentrations of PhoB tested (10–100  $\mu\text{M}$ ), and the rate of transfer from P-VanS to PhoB versus P-VanS concentration was linear over the concentrations of P-VanS employed (0.05–0.5  $\mu\text{M}$ ). The rate versus [PhoB] plot follows a profile that is consistent with saturable, rectangular hyperbola kinetics (see Figure 4). This suggests that the phosphotransfer reaction proceeds through an initial complex formation, followed by a chemical transfer step which would be rate-limiting (eq 2). Due to limiting solubilities of PhoB



( $\leq 120 \mu\text{M}$ ), it was not possible to measure the rate of transfer under saturating conditions; however, by fitting the data to a rectangular hyperbola model, a first-order rate constant of  $k_{\text{transfer}} = 0.20 \pm 0.04 \text{ min}^{-1}$  ( $k_2$ ) was obtained, with an apparent Michaelis constant of  $K_{\text{M,PhoB}} = 100 \pm 35 \mu\text{M}$ . The kinetic constants obtained from these studies are consistent with rapid equilibrium kinetics, where the encounter complex [P-VanS·PhoB] is in rapid equilibrium with the dissociated proteins, as the maximal rate of transfer is relatively slow ( $k_{\text{transfer}}$ ) and the Michaelis constant for the transfer is relatively high ( $K_{\text{M,PhoB}}$ ). Under these conditions, where the rate of transfer is likely to be much slower than the rate of dissociation ( $k_2 \ll k_{-1}$ ), the  $K_{\text{M,PhoB}}$  is a measure of the actual dissociation constant for the two proteins.

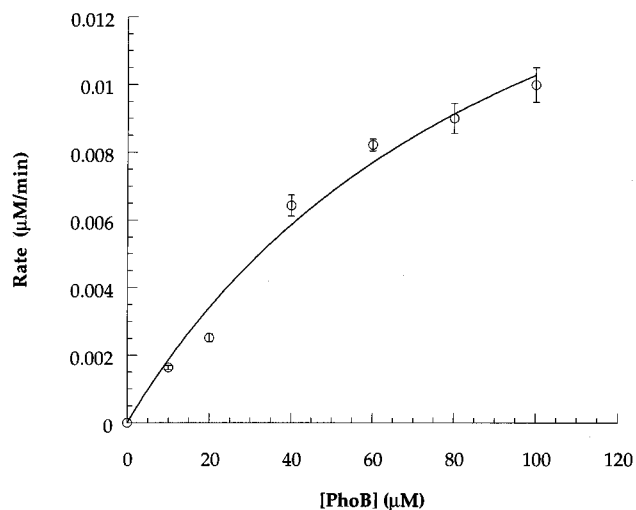
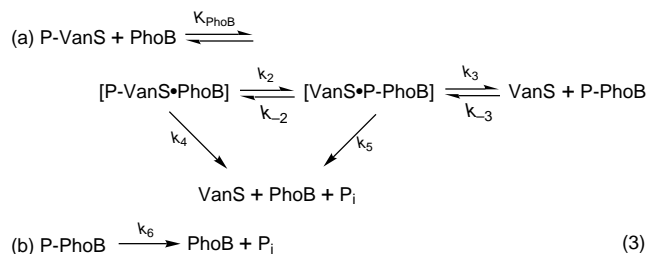


FIGURE 4: Saturation curve of  $^{32}\text{P}$ -VanS to PhoB phosphotransfer. The data were collected under initial conditions as described in Materials and Methods and fit to a rectangular hyperbola (solid line).

*Simulation of the  $^{32}\text{P}$ -VanS to PhoB Phosphotransfer Reaction.* On the basis of the data collected from VanS and PhoB phosphotransfer studies, we proposed a minimal model for the phosphotransfer reaction between VanS and PhoB (see eq 3). This proposal incorporates the elements described



in eq 2 as well as several pathways for generation of phosphate in the phosphotransfer reaction. In this model,  $\text{P}_i$  may be derived from three independent sources: (a) P-PhoB, (b) the [VanS·P-PhoB] complex, or (c) the [P-VanS·PhoB] complex. Phosphate produced from species a or b would be expected at the rates measured in the dephosphorylation studies on P-PhoB; therefore, the hydrolysis pathway from the [P-VanS·PhoB] complex was proposed to account for the accumulation of  $\text{P}_i$  produced in the early stages of the reaction. In effect, this pathway represents a branching point for the phosphotransfer reaction, where direct hydrolysis competes with PhoB for P-VanS. Finally, the biphasic character of the phosphotransfer time course could be attributable to equilibration between the forward and reverse reactions. The proposed model accounts for this possibility, through a reversible transfer of phosphate between the two protein complex species. As a test of the model, a kinetic simulation was performed which incorporated all of the elements of the proposed model and the experimentally determined constants. The results of the simulation for the forward and backward reactions are shown in Figures 1 and 3 (solid lines), respectively, and closely predict the behavior of the forward and backward reactions of the phosphotransfer reaction over the entire time course.

*Phosphotransfer Kinetics from  $^{32}\text{P}$ -VanS to VanR.* Earlier work on VanS and VanR had demonstrated that the phosphotransfer between these two proteins was extremely

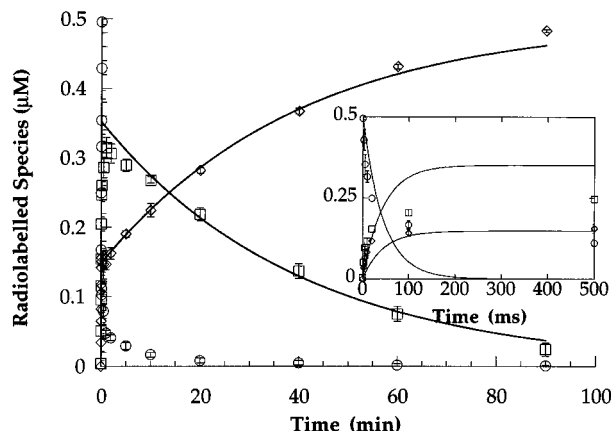


FIGURE 5: Time course of phosphotransfer from  $^{32}\text{P}$ -VanS to VanR. Reactions were run and analyzed using SDS-PAGE and phosphorimager analysis as described in Materials and Methods. Data at designated time points represent  $^{32}\text{P}$ -labeled species: ( $\circ$ ) P-MBP-VanS; ( $\square$ ) P-VanR, and ( $\diamond$ ) inorganic  $\text{P}_i$ . Inset graph corresponds to data collected using rapid quench kinetics. Solid lines represent computer simulations according to the phosphotransfer model (see eq 5). Initial concentrations of species were set as follows: P-MBP-VanS,  $0.5\ \mu\text{M}$ ; MBP-VanS,  $4.5\ \mu\text{M}$ ; VanR,  $15\ \mu\text{M}$ . Simulations were run with the following kinetic constant values:  $K_{\text{M,VanR}} = 30\ \text{nM}$ ;  $k_2 = 95\ \text{min}^{-1}$ ;  $k_{-2} = 0.001\ \text{min}^{-1}$ ;  $k_3 = 120\ \text{min}^{-1}$ ;  $k_{-3} = 1\ \mu\text{M}^{-1}\ \text{min}^{-1}$ ;  $k_4 = 0.01\ \text{min}^{-1}$ ;  $k_5 = 0.025\ \text{min}^{-1}$ ;  $k_6 = 40\ \text{min}^{-1}$ ;  $K_{\text{VanS/R}} = 30\ \text{nM}$ . Rate constants  $k_{-2}$ ,  $k_3$ , and  $k_{-3}$  were derived empirically and found to be relatively insensitive to the overall fit; all other constants were used as reported (Wright et al., 1993) or measured as described in Materials and Methods.

rapid: near complete phosphotransfer was observed in  $<10$  s (Wright et al., 1993; Fisher et al., 1995). These results prompted us to study the phosphotransfer reaction on the millisecond time scale using rapid chemical quench techniques. These methods allowed for analysis of the phosphotransfer reactions under conditions identical to those employed for the  $^{32}\text{P}$ -VanS to PhoB phosphotransfer experiments; however, optimal results were obtained when the protein concentrations were reduced 4-fold ( $^{32}\text{P}$ -VanS  $0.5\text{ }\mu\text{M}$ ; VanR  $15\text{ }\mu\text{M}$ ). Under these conditions, maximal transfer occurred within about 100 ms, well within the reaction time limits of the rapid quench apparatus ( $\geq 2$  ms). The reaction time course obtained using these methods is shown in Figure 5. While it is clear from the time course that VanS is far more efficient in phosphotransfer to VanR than PhoB, the overall reaction profiles obtained for the two response regulators share several common elements. First, the  $^{32}\text{P}$ -VanS to VanR phosphotransfer time course follows a biphasic process that is characterized by an early phase (0–30 s) of rapid depletion of phosphate label from VanS with a corresponding rise in both P-VanR and  $\text{P}_i$  to give a maximal loading of P-VanR to  $\approx 60\%$  of the initial  $^{32}\text{P}$ -VanS. This early phase is followed by a slow hydrolysis of P-VanR to inorganic phosphate (1–90 min). As with the P-VanS to PhoB phosphotransfer reaction, an early accumulation of  $\text{P}_i$  was observed. Previous work on purified P-VanR (Wright et al., 1993) has shown that it has a relatively long lifetime under these conditions ( $t_{1/2} = 820 \pm 240$  min) even in the presence of excess VanS ( $t_{1/2} = 120 \pm 40$  min). Therefore, it is unlikely that the initial accumulation of  $\text{P}_i$  is produced from this species alone.

The  $^{32}\text{P}$ -VanS to VanR phosphotransfer reaction was also studied under initial conditions similar to those employed for PhoB. The reaction was well behaved kinetically, as the

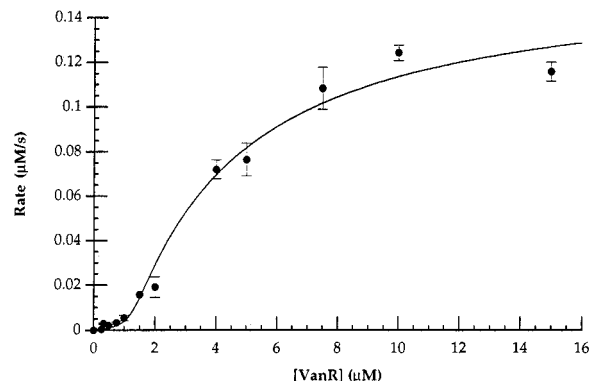
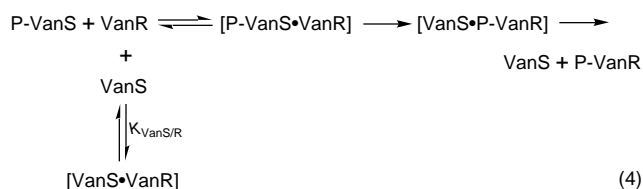


FIGURE 6: Saturation curve of  $^{32}\text{P}$ -VanS to VanR phosphotransfer. The data were collected under initial conditions as described in Materials and Methods and fit to a substrate depletion model (solid line, see eq 4).

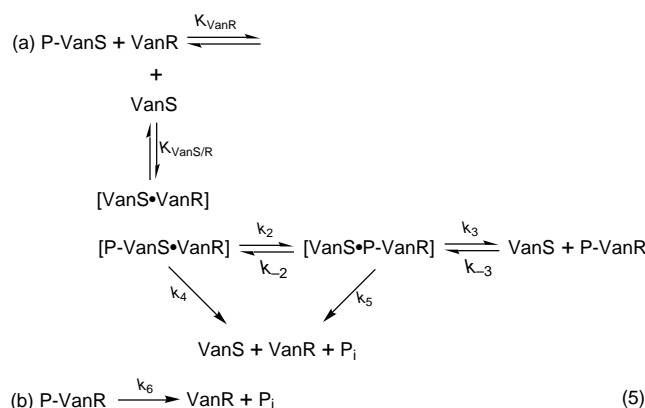
P-VanR accumulation was found to be linear to  $\approx 15\%$  of the reaction progress ( $\approx 30\%$  P-VanS consumption,  $\approx 15\%$  P-VanR formed) over the range of VanR concentrations tested ( $0.5\text{--}15\text{ }\mu\text{M}$ ), and the rate of transfer was linear with P-VanS concentration ( $0.1\text{--}0.5\text{ }\mu\text{M}$ ). The reaction was found to be saturable at high VanR concentrations ( $7.5\text{--}15\text{ }\mu\text{M}$ ); however, the saturation curve was sigmoidal (see Figure 6). These results clearly show that the two proteins form a complex prior to chemical transfer; however, a sigmoidal saturation curve is inconsistent with the simple rapid equilibrium model demonstrated by the P-VanS to PhoB phosphotransfer reaction. Sigmoidal saturation curves are expected in cases where the substrate interacts with an inhibitor, resulting in a depletion of the free substrate (Segel, 1993). These results prompted us to investigate potential inhibitors of VanR in our assay. Since our preparations of  $^{32}\text{P}$ -VanS are inherently contaminated with free VanS (1:9 ratio), we suspected that the free VanS was inhibiting the VanR by forming a nonproductive complex (see eq 4). This hypoth-



esis was supported by the observation that the phosphotransfer rate was inversely proportional to the free VanS concentration (data not shown). The saturation curve was then fit according to a substrate depletion model using a rectangular hyperbola which was dependent on the calculated free substrate concentration based on three variables: the dissociation constant of the [VanS•VanR] complex ( $K_{\text{VanS/R}}$ ), the Michealis constant of the [P-VanS•VanR] complex ( $K_{\text{M,VanR}}$ ), and the first-order phosphotransfer rate ( $k_{\text{xfer}}$ ). A reasonable fit was obtained using this model to give the following values:  $K_{\text{M,VanR}} = 3.61 \pm 0.818 \mu\text{M}$ ,  $k_{\text{xfer}} = 96 \pm 7.9 \text{ min}^{-1}$ , and  $K_{\text{VanS/R}} = 0.032 \pm 0.051 \mu\text{M}$ . Interestingly, the dissociation constant for VanR with free VanS was found to be  $\approx 100$ -fold smaller than that calculated for the phosphoform. While it is possible that the two forms of VanS have such different affinities for VanR, the discrepancy between the two values may result from the rapid phosphotransfer kinetics. Whereas the dissociation constant calculated for the free VanS interaction with VanR is based solely on the

protein complex formation, the Michealis constant obtained for P-VanS with VanR is a function of the phosphotransfer reaction. The fast rate of transfer, coupled with the tight complex formation, suggests that the phosphotransfer reaction is not under rapid equilibrium. In this case, the apparent equilibrium constant for the P-VanS•VanR complex would be a function of the forward transfer rate and the protein complex association rate ( $K_{M,VanR} \approx k_2/k_1$ ), rather than the ratio of the complex association and dissociation rates. As a result, the value of  $\approx 30$  nM obtained for free VanS is likely to be a more accurate estimate of the true dissociation constant of the VanS-VanR interaction.

**Simulation of the  $^{32}\text{P}$ -VanS to VanR Phosphotransfer Reaction.** We proposed a model similar to that used in the P-VanS to PhoB phosphotransfer reaction for the phosphotransfer from  $^{32}\text{P}$ -VanS to VanR (see eq 5); the only



difference between the two schemes was the inclusion of the competing inhibition by VanS by a nonproductive VanS•VanR complex formation. A simulation of the reaction time course was performed to test this model, and the results are shown in Figure 5 (solid lines). The simulation very closely predicts the phosphotransfer reaction time course in both the early phase (to  $\approx 80\%$  completion) and the slow decay of P-VanR; however, the simulation does not fit an intermediate phase reaction ( $\approx 50$  ms to 5 min). This phase accounts for  $\approx 20\%$  of the initial P-VanS which exhibits a slow transfer to VanR. The difficulty in fitting the intermediate phase of the reaction may be related to the preparation of VanS as an MBP fusion protein.  $^{32}\text{P}$ [MBP-VanS] is known to form a number of oligomeric states, as assessed by native PAGE (Z. Wu and C. T. Walsh, unpublished data), and it is possible that these states have different reactivities in the phosphotransfer reaction and are kinetically trapped by VanR. The fact that the reaction reaches completion (all P-MBP-VanS is consumed) implies that these states are either capable of transfer or are in equilibrium with species that are competent in the phosphotransfer reaction.

**Inhibition of Phosphotransfer from  $^{32}\text{P}$ -VanS to VanR by PhoB.** The kinetic studies performed with  $^{32}\text{P}$ -VanS and the two response regulators under initial conditions not only provide a quantitative estimate for the overall efficiency and specificity of phosphotransfer but also can be used to analyze potential inhibitors of the phosphotransfer process. To demonstrate this potential, as well as to provide supporting data for the current model, we tested whether PhoB could act as an inhibitor of the phosphotransfer reaction between P-VanS and VanR. This application is particularly challenging, since both the VanR and PhoB are substrates for

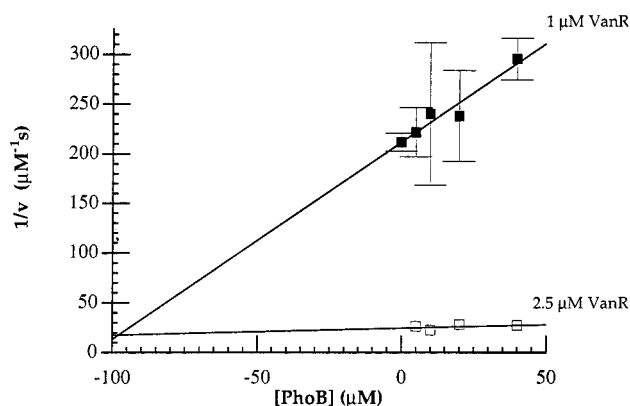
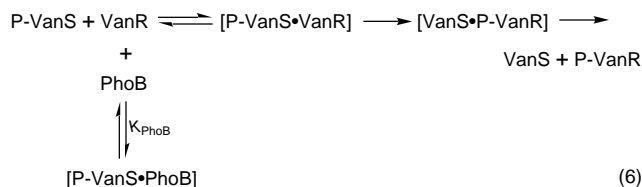


FIGURE 7: Dixon plot of PhoB inhibition of  $^{32}\text{P}$ -VanS to VanR phosphotransfer.

VanS, and they are almost identical in molecular mass ( $\approx 26$  500 kDa). As a result, the two proteins will comigrate on SDS-PAGE and phosphoprotein mixtures cannot be analyzed directly using the current assay. However, on the short reaction times ( $\approx 75$  ms) used in the P-VanS to VanR phosphotransfer reactions, PhoB would be expected to act only as a competitive inhibitor of P-VanR formation rather than as a substrate for  $^{32}\text{P}$ -VanS (PhoB  $k_{\text{xfer}} = 0.2 \text{ min}^{-1}$ , see eq 6). Indeed, PhoB-dependent inhibition of the P-VanS



to VanR phosphotransfer reaction was observed and a Dixon analysis of the inhibition was performed (see Figure 7). The Dixon plot is consistent with competitive inhibition with a calculated  $K_i = 95 \pm 30 \mu\text{M}$ . In addition, the P-VanS to VanR phosphotransfer kinetic constant values (calculated from the slopes of the plot) are in agreement with the values obtained from the saturation kinetics studies ( $K_{M,VanR} = 1\text{--}10 \mu\text{M}$ ;  $k_{\text{xfer}} \approx 60 \text{ min}^{-1}$ ).

## DISCUSSION

Two-component signal transduction systems have recently received considerable attention due to their widespread occurrence as well as for potential targets of antibacterial therapeutic agents (Alex & Simon, 1994; Swanson et al., 1994). In spite of this, there have been relatively few investigations into the factors that govern the rates and specificities of phosphotransfer reactions for these proteins. Detailed investigations on the interactions between two-component system proteins have been hindered by a number of factors including (a) difficulties in the preparation of large quantities of the purified proteins, (b) fast phosphotransfer kinetics, and (c) short-lived phosphorylated protein intermediates. As a result, investigations on the phosphorylation kinetics of the response regulator class have focused on reactions with small molecule phosphodonors [e.g., acetyl phosphate (Stock et al., 1995)] or have been limited to kinetic simulations of the overall phosphotransfer process (Lukat et al., 1991; Bray et al., 1993; Morrison & Parkinson, 1994; Hauri & Ross, 1995).

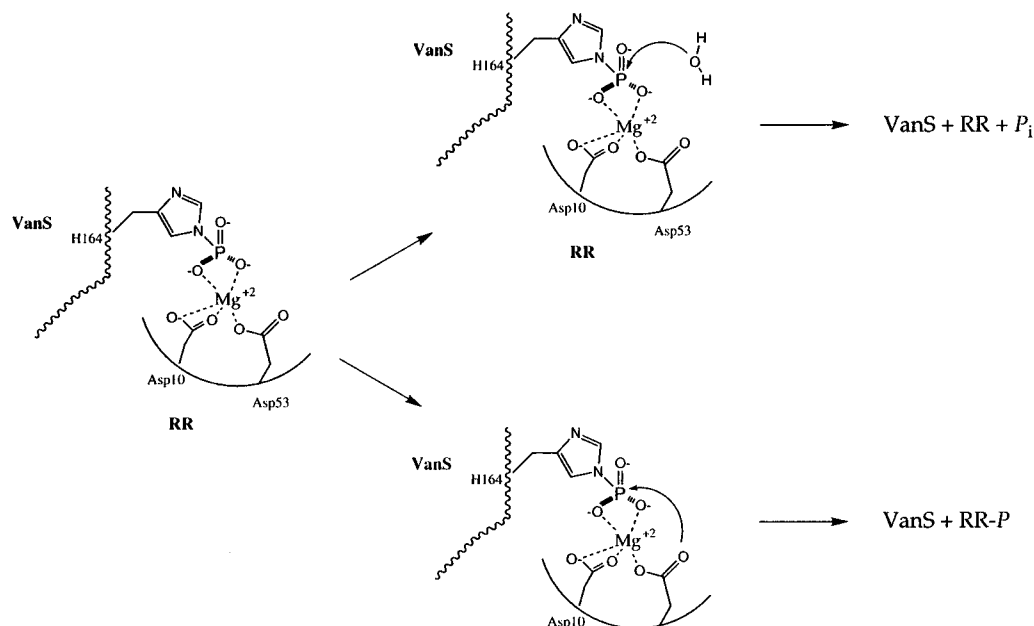


FIGURE 8: Proposed mechanism for competing phosphate hydrolysis pathway.  $\text{Mg}^{2+}$  coordination geometry was based on comparisons to the structural data on CheY (Volz, 1993); additional coordination by Asp9 (VanR) was not shown for clarity.

Our interests in the development of *in vivo* models of the *Enterococcus faecium* vancomycin resistance two-component system (VanS/VanR) through the heterologous cross-talk interaction between the sensor kinase VanS and the *E. coli* response regulator PhoB (Fisher et al., 1995) led us to investigate the differences in reactivities between the cognate and the heterologous systems. In this work, we have performed a detailed kinetic analysis of the phosphotransfer reactions between the sensor kinase VanS and two response regulator proteins, its homologous partner VanR and PhoB as a heterologous partner. To our knowledge, these studies represent the most comprehensive analyses to date on the phosphorylation kinetics between a sensor kinase and response regulator proteins.

The kinetic data collected under initial conditions for both response regulators show that the response regulators form detectable complexes with  $^{32}\text{P}$ -VanS prior to phosphotransfer and that chemical transfer is the rate-limiting step. These results contrast with mechanistic studies performed on response regulator proteins with small-molecule phosphate donors (acetyl phosphate, etc.), which found, not surprisingly, that substrate binding of these nonspecific substrates is relatively weak ( $K_M \approx \text{mM}$ ) and rate-limiting (Stock et al., 1995). The differences in kinetic behavior between the sensor kinase and the small-molecule phosphodonors are most likely due to specific protein–protein interactions between the sensor kinase and the response regulators that are not present in the low molecular weight phosphodonor molecules. The dissociation constant of 30 nM obtained in these experiments for MBP-VanS interacting with VanR is consistent with estimates of the VanS•VanR complex formation obtained from previous studies on DNA binding experiments with VanR (Holman et al., 1994). These studies demonstrated that VanS was an efficient competitor for DNA binding ( $\text{IC}_{50} = 1 \mu\text{M}$ ; VanR =  $2.7 \mu\text{M}$ ), suggesting that the actual dissociation constant is less than  $1 \mu\text{M}$ . Tight complexes of response regulator and sensor kinase proteins have been observed in at least one other system; biophysical measurements on the related chemotaxis two-component

system have shown that the sensor protein (CheA) and response regulator (CheY) form a complex in the nanomolar range [ $\approx 30 \text{ nM}$  (Shuster et al., 1993)]. Finally, protein–protein interactions in the bacterial phosphoenol pyruvate/glycose phosphotransferase system (PTS) have been measured in the micromolar range (Waygood & Steeves, 1980; Weigel et al., 1982). While it is not a canonical two-component system, the PTS also catalyzes phosphoryl transfer between two proteins via histidine–phosphate intermediates.

It has been proposed that protein-specific interaction domains on both the sensor kinase and response regulator proteins provide a means for regulating the specificity (“cross-talk”) between signal transduction systems (Kofoid & Parkinson, 1988; Parkinson & Kofoid, 1992; Volz, 1993), and these interactions may account for the observed differences in the kinetics between the two response regulator proteins. A comparison of the apparent Michaelis–Menten constants for the two response regulators ( $K_{M,\text{VanR}} \approx 3.61 \mu\text{M}$ ;  $K_{M,\text{PhoB}} \approx 100 \mu\text{M}$ ) shows an  $\approx 30$ -fold binding preference for VanR over PhoB for VanS. The first-order transfer rates for the two proteins are even more disparate (VanR  $k_{\text{xfer}} \approx 96 \text{ min}^{-1}$ ; PhoB  $k_{\text{xfer}} = 0.2 \text{ min}^{-1}$ ), representing a  $\approx 500$ -fold rate enhancement for the homologous over the heterologous system. Taken together, these differences indicate  $\geq 10^4$ -fold difference in reactivity for the homologous VanR system over the heterologous PhoB/VanS system. The fact that the two proteins share  $>35\%$  sequence identity, as well as near superposable circular dichroism spectra (data not shown), indicates that the pronounced specificity of VanS for the two proteins is not due to gross structural differences between PhoB and VanR. Rather, it is likely that the two proteins have the same molecular scaffold but have evolved specific protein surface contacts to discriminate between the several sensor kinases present in the cellular milieu. These conclusions are in accord with our attempts to demonstrate cross-talk between VanS and response regulators other than PhoB. We have overexpressed several response regulator proteins which had significant sequence identity to VanR:



ArcA (40%), OmpR (40%), and CreB (36%). We were unable to detect any cross-talk as assayed by  $^{32}\text{P}$ -transfer between VanS and these response regulators (data not shown), despite the fact that all of these proteins (including PhoB) are closely related members of the OmpR subfamily of response regulator proteins (Stock et al., 1989).

The results from the phosphotransfer time course studies have other mechanistic implications. In the time courses for both response regulators, a rapid accumulation of inorganic phosphate was observed in the early stages of the reaction. This phosphate production could not be attributed to dephosphorylation of the phosphorylated response regulator but was more consistent with a branched phosphotransfer pathway where direct hydrolysis competes with the response regulator for phosphotransfer. The prototypic mechanism for the response regulator phosphotransfer reaction, based on structural analyses of the response regulator protein CheY, is proposed to involve activation of histidyl-phosphate group of the sensor kinase by chelation to the response regulator-bound divalent metal cation ( $\text{Mg}^{2+}$ ) as shown in Figure 8 (Stock et al., 1995). In this regard, the metal cation serves as a template for the reaction, and the phosphotransfer proceeds through attack by the response regulator aspartate side chain on the activated phospho-His of the sensor. The concomitant increase in inorganic phosphate with phosphorylated response regulator suggests that, in addition to attack by the response regulator aspartate group, the activated phosphate group is also susceptible to attack by a water molecule (potentially activated by the  $\text{Mg}^{2+}$  cation as well) (Figure 8). Comparisons of the rates of transfer for these two processes suggests that this alternative pathway accounts for about 25% of the flux with both VanR and PhoB as partners.

The demonstration of inhibition of the P-VanS to VanR phosphotransfer reaction by PhoB illustrates the ability to screen and quantitatively assess inhibitors of the phosphotransfer reaction and could provide an avenue for the identification of new agents which block the signal transduction pathway. Moreover, the inhibition constants obtained in these studies also provide a useful, independent measure of the binding interactions between PhoB and VanS. These studies, along with measurements of the rate of initial phosphate accumulation upon phosphotransfer and the kinetic constants derived from studies under initial conditions, provide reliable parameters for evaluation of the factors that govern the response regulator recognition by VanS. Further, the *in vivo* activation of PhoB by VanS (Fisher et al., 1995) should provide a convenient system for screening and isolation of PhoB mutants with altered specificity (e.g., increased) to VanS. Taken together, these approaches should serve both to identify the interaction domains and allow a quantitative evaluation of the contributions of the key residues to phosphotransfer reactivity.

## ACKNOWLEDGMENT

We thank Dr. Gregory Tucker-Kellogg for assistance in the kinetic simulations, Drs. Simon Lynch and Ed C. C. Lin

for preparations of purified ArcA protein, and Dr. Philip A. Cole for helpful suggestions and comments.

## REFERENCES

- Alex, L. A., & Simon, M. I. (1994) *Trends Genet.* 10, 133–138.
- Arthur, M., Molinas, C., & Courvalin, P. (1992) *J. Bacteriol.* 174, 2582–2591.
- Barshop, B. A., Wrenn, R. F., & Frieden, C. (1983) *Anal. Biochem.* 130, 134–145.
- Bray, D., Bourret, R. B., & Simon, M. I. (1993) *Mol. Biol. Cell.* 4, 469–482.
- Fisher, S. L., Jiang, W., Wanner, B. L., & Walsh, C. T. (1995) *J. Biol. Chem.* 270, 23143–23149.
- Gill, S. C., & von Hippel, P. H. (1989) *Anal. Biochem.* 182, 319–326.
- Hakenbeck, R. (1994) in *Bacterial Cell Wall* (Ghuysen, J.-M., & Hakenbeck, R., Eds.) pp 535–546, Elsevier, New York.
- Hauri, D. C., & Ross, J. (1995) *Biophys. J.* 68, 708–722.
- Holman, T. R., Wu, Z., Wanner, B. L., & Walsh, C. T. (1994) *Biochemistry* 33, 4625–4631.
- Kamberov, E. S., Atkinson, M. R., Chandran, P., & Ninfa, A. J. (1994) *J. Biol. Chem.* 269, 28294–28299.
- Kofoid, E. C., & Parkinson, J. S. (1988) *Proc. Natl. Acad. Sci. U.S.A.* 85, 4981–4985.
- Kunkel, T. A. (1985) *Proc. Natl. Acad. Sci. U.S.A.* 82, 488–492.
- Lukat, G. S., Lee, B. H., Mottenen, J. M., Stock, A. M., & Stock, J. B. (1991) *J. Biol. Chem.* 266, 8348–8354.
- Morrison, T. B., & Parkinson, J. S. (1994) *Biotechniques* 17, 920–926.
- Nagarajan, R. (1991) *Antimicrob. Agents Chemother.* 35, 605–609.
- Parkinson, J. S. (1993) *Cell* 73, 857–871.
- Parkinson, J. S., & Kofoid, E. C. (1992) *Annu. Rev. Genet.* 26, 76–112.
- Rudolph, J., Tolliday, N., Schmitt, C., Schuster, S. C., & Oesterhelt, D. (1995) *EMBO J.* 14, 4249–4257.
- Segel, I. H. (1993) *Enzyme Kinetics*, pp 203–206, John Wiley & Sons, New York.
- Shuster, S. C., Swanson, R. V., Alex, L. A., Bourret, R. B., & Simon, M. I. (1993) *Nature* 365, 343–347.
- Spratt, B. G., Hedge, P. J., te Heesen, S., Edelman, A., & Broome-Smith, J. K. (1986) *Gene* 41, 337–342.
- Stock, J. B., Ninfa, A. J., & Stock, A. M. (1989) *Microbiol. Rev.* 53, 450–490.
- Stock, J. B., Surette, M. G., Levit, M., & Park, P. (1995) in *Two-Component Signal Transduction* (Hoch, J. A., & Silhavy, T. J., Eds.) pp 25–52, ASM Press, Washington, D.C.
- Studier, F. W. (1991) *J. Mol. Biol.* 219, 37–44.
- Swanson, R. V., Alex, L. A., & Simon, M. I. (1994) *Trends Biochem. Sci.* 19, 485–490.
- Tokishita, S.-I., Kojima, A., & Mizuno, T. (1992) *J. Biochem. (Tokyo)* 111, 707–713.
- Volz, K. (1993) *Biochemistry* 32, 11741–11753.
- Wanner, B. L. (1993) *J. Cell. Biochem.* 51, 47–54.
- Wanner, B. L., & Chang, B.-D. (1987) *J. Bacteriol.* 169, 5569–5574.
- Waygood, E. B., & Steeves, T. (1980) *Can. J. Biochem.* 58, 40–48.
- Weigel, N., Waygood, E. B., Kukuruzinska, M. A., Nakazawa, A., & Roseman, S. (1982) *J. Biol. Chem.* 257, 14461–14469.
- Wilheim, M. P. (1991) *Mayo Clin. Proc.* 66, 1165–1170.
- Wright, G. D., & Walsh, C. T. (1992) *Acc. Chem. Res.* 25, 468–473.
- Wright, G. D., Holman, T. R., & Walsh, C. T. (1993) *Biochemistry* 32, 5057–5063.